Chowdhury et al., https://doi.org/10.1083/jcb.201608063

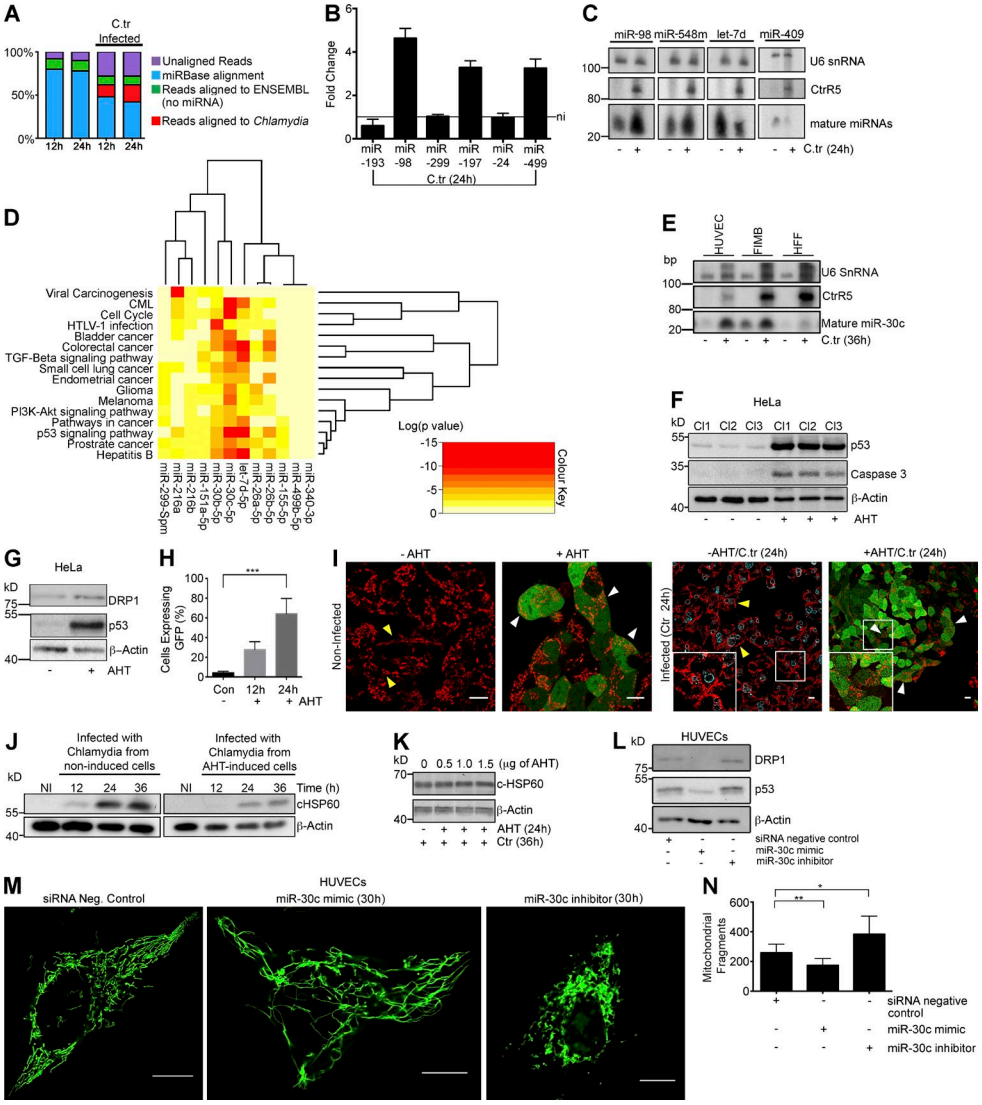

Figure S1. **Analysis and validation of the miRNA deep sequencing data; infectivity assays of chlamydial infection in HUVECs after artificial modulation of miR-30c; validation of miR-30c mimic, inhibitor, and sponge; and effect of miR-30c modulation on the mitochondrial network of HeLa sponge cells and HUVECs.** (A) Read distribution of RNA sequencing data. Mature miRNA were mapped against the miRBase database, and other human and chlamydial genes were mapped to the complete human and chlamydial genomes. (B and C) Specific miRNAs were validated by qRT-PCR or Northern blot of noninfected HUVECs against HUVECs infected with *C. trachomatis* (C.tr) for 24 h. U6 snRNA was used as endogenous control for qRT-PCR. Fold changes were normalized to the control noninfected cells grown for 24 h, represented as the black bar. U6 snRNA was used as loading control, and CtrR5 was used as a marker for chlamydial infection in the Northern blot. (D) Binary heat map of significance level–based clustering of miRNA and signaling pathways by DIANA-miRPath v2.0 web-server. All pathways targeted significantly are represented in deeper colors. The dendrogram on the miRNA right axis clusters together miRNAs that target similar pathways. (E) Northern blot of total RNA from infected and noninfected HUVEC, hFIMB, and HFF cells probed against miR-30c, U6snRNA, and chlamydial small RNA CtrR5. (F and G) Several single-cell clones of HeLa cells were tested for expression of miR-30c sponge by immunoblotting the protein lysates to check for up-regulation of the miR-30c targets p53, caspase 3, and Drp1. (H) Graph represents the rate of sponge induction after 24 h of anhydrous tetracycline treatment indicated by GFP expression (green; 509 nm). (I) GFP-positive cells were counted using Object Count from micrographs of induced miR-30c sponge cells stained with MitoTracker Deep Red FM. White box indicates enlargements. White arrows indicate fragmented mitochondria and yellow arrows indicate unfragmented mitochondria in a noninduced cell. (J) Immunoblot of infectivity assays of 36 h of primary *C. trachomatis* infection in induced and noninduced miR-30c sponge HeLa cells. Blots were probed with antibodies against cHSP60 and β-actin. (K) Immunoblot of HeLa cells treated with AHT and infected with *C. trachomatis* for 24 h against cHSP60 and β-actin. (L) Immunoblot of HUVECs transfected with siRNA negative control, miR-30c mimic, and inhibitor. The blots were probed with antibodies against p53, Drp1, and β-actin. (M) Micrographs show the effect of artificial modulation of miR-30c on HUVEC mitochondrial network. HUVECs expressing mitochondrial presequence–tagged GFP were transfected with siRNA negative control, miR-30c mimic, or inhibitor for 24 h before imaging. Bars, 10 µm. (N) Graph represents quantification of the number of mitochondrial fragments in HUVECs 30 h after transfection with siRNA negative control, miR-30c mimic, or inhibitor (number of experiments $n = 5$; ~20 cells were analyzed per experiment). All data represent mean ± SD. Asterisks denote significance by unpaired *t* test: *, $P < 0.05$; **, $P < 0.01$; ***, $P < 0.001$.

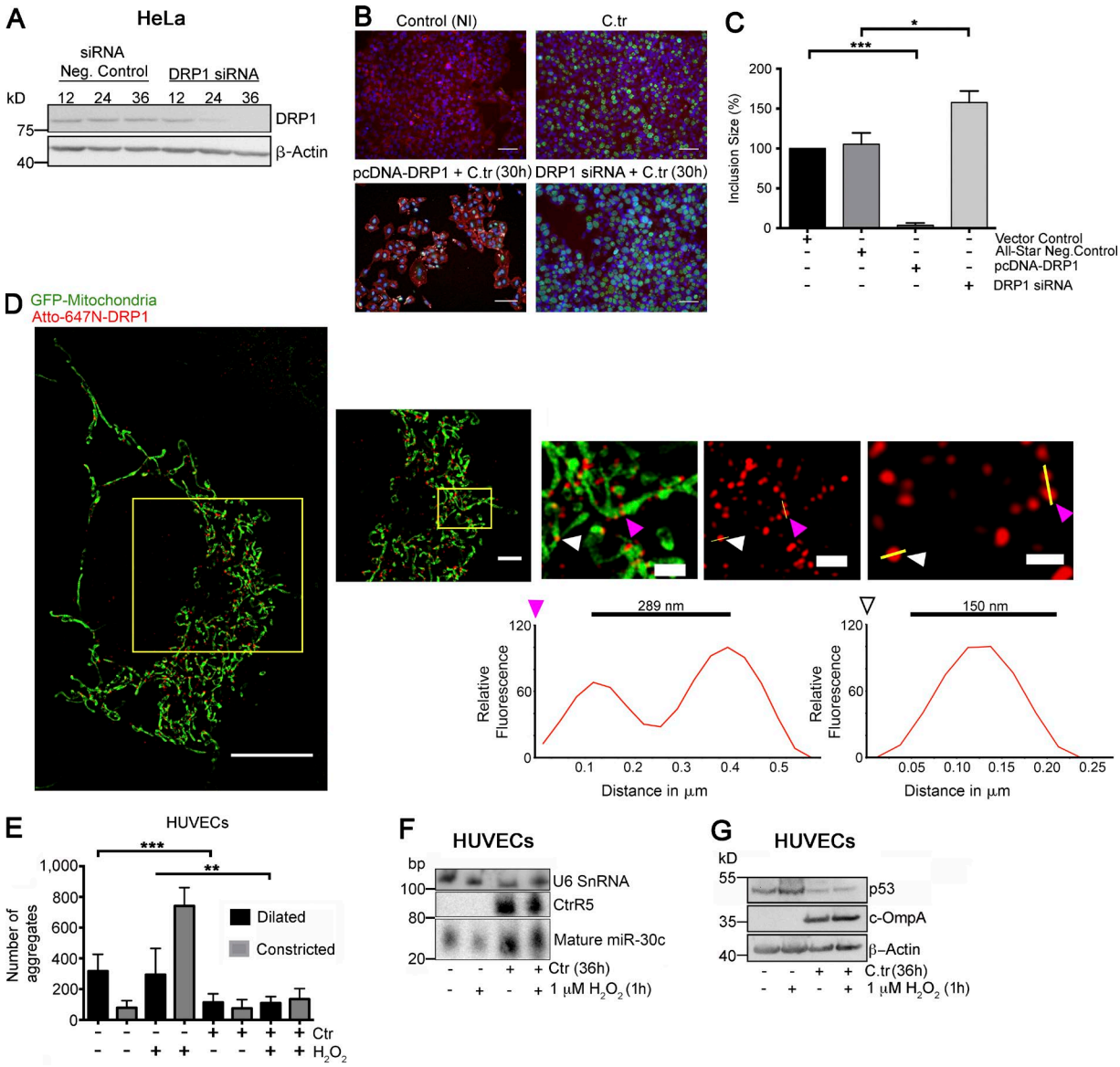

Figure S2. **Structural analysis of Drp1 rings by SR-SIM, HUVECs transfected with DRP1 siRNA, and overexpression vector and Operetta-based quantification of *C. trachomatis* inclusion sizes after artificial modulation of Drp1; effect of H_2O_2 treatment on miR-30c and p53 levels in noninfected and *C. trachomatis*–infected HUVECs and standardization of Drp1 siRNA in HeLa cells.** (A) Quantification of the efficiency of siRNA-mediated knockdown of DRP1 in HeLa cells. Cells were transfected with AllStars–negative siRNA control or DRP1 siRNA for 12, 24, and 36 h and lysed for analysis by Western blot. (B) Representative images of Operetta-based quantification of *C. trachomatis* (C.tr) inclusion sizes in HUVECs transfected with Drp1 siRNA or Drp1 overexpression vector. The transfected and nontransfected cells were infected with *C. trachomatis* expressing GFP for 30 h. Bars, 30 µm. (C) Graph represents the quantification of chlamydial inclusion sizes from control (vector control or AllStars negative control) or cells transfected with Drp1 overexpression vector or Drp1 siRNA (n = 3). (D) Structured illumination micrograph of H_2O_2 treated HUVECs expressing GFP targeted to the mitochondria. Bar, 10 µm. Drp1 was stained with Atto-647N. Enlargement (yellow boxes) exhibit two states of Drp1 rings. Bar, 2.5 µm. A constricted ring is marked with a white arrowhead, and a dilated ring is marked with a pink arrowhead. Bars, 0.5 µm. Intensity profile plots (along the yellow line through the aggregates) of these two rings are plotted as graphs. Diameter of a dilated ring is measured to be ~289 ± 70 nm (n = 616) and a constricted ring, ~150 ± 46 nm (n = 442) along the yellow bar drawn through the aggregates. (E) Graph represents quantification of the dilated and constricted fractions of Drp1 aggregates in *C. trachomatis*–infected and uninfected HUVECs. Indicated samples were treated with 1 µM H_2O_2 for 1 h or posttreated with 1 µM H_2O_2 for 1 h after 24 h of *C. trachomatis* infection; ~6 (0.8 × 0.8-µm) sections were analyzed from each cell. 15 cells were chosen from a random selection of ~5 regions of interest in each sample (n = 10). (F) Northern blot of RNA isolated from noninfected and *C. trachomatis* –infected HUVECs treated with 1 µM H_2O_2 for 1 h. The blot was probed for U6 SnRNA, miR-30c, and CtrR5. (G) Immunoblot of noninfected and *C. trachomatis*–infected HUVEs treated with 1 µM H_2O_2 for 1 h. The blot was probed for p53, c-OmpA, and β-actin. All data represent mean ± SD. Asterisks denote significance by one-way analysis of variance followed by multiple comparisons test for panel E and by unpaired t test for panel C: *, $P < 0.05$; **, $P < 0.01$; ***, $P < 0.001$; ns, nonsignificant.

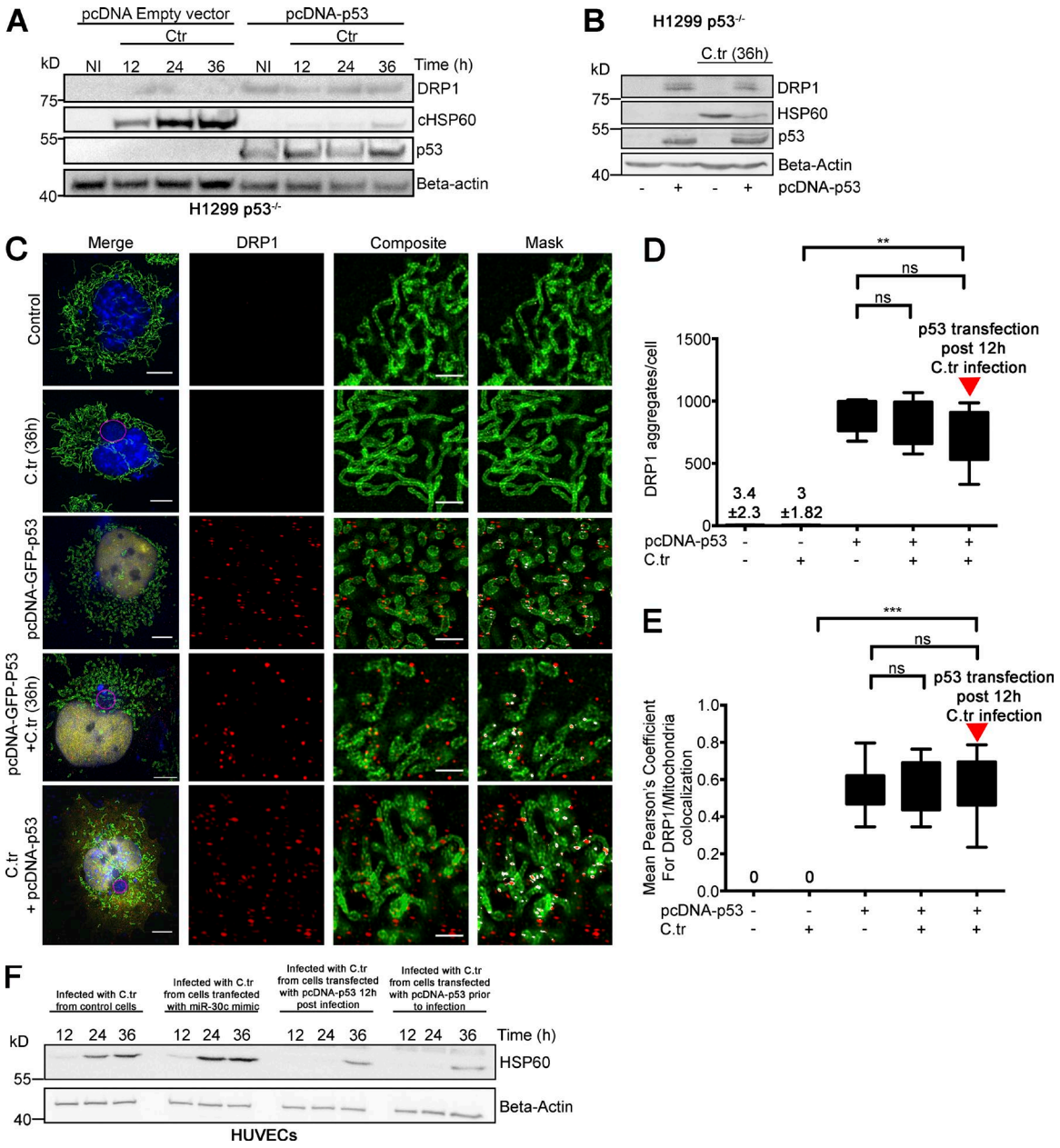

Figure S3. **Drp1 expression and mitochondrial morphology and infectivity assays of primary chlamydial infection in HUVECs transfected with miR-30c mimic siRNA and p53 overexpression vector.** (A) Immunoblots for different durations of *C. trachomatis* (C.tr) infection in control H1299 p53$^{-/-}$ cells and H1299 p53$^{-/-}$ cells transfected with a p53 overexpression vector (Marin et al., 2000). Blots were probed for Drp1, p53, cHSP60, and β-actin (n = 3). (B) Immunoblots for 12 h of *C. trachomatis* infection before control vector and p53 overexpression vector transfection. *C. trachomatis* was then allowed to grow for another 24 h before lysis. Blots were probed for Drp1, p53, cHSP60, and β-actin (n = 3). (C) Structured illumination micrograph of HUVECs infected with *C. trachomatis* for 36 h, transfected with pcDNA-GFP-p53 overexpression vector, or both. Indicated cells were infected with *C. trachomatis* for 12 h before transfection and then allowed to grow for another 24 h after transfection. The cells express p53 tagged with GFP (yellow) and were stained for Drp1 (red) and Tom20 (green) to mark the mitochondria. Cellular nucleus and chlamydial nuclear material is stained with DAPI (blue) and encircled by the pink ellipse. Bars, 10 µm. Insets are 10 × 10-µm regions selected for colocalization analysis. Inset marked mask shows regions of overlap between Drp1 and mitochondrial Tom20 signal in white. Bars, 2 µm. (D) Graph represent quantification of Drp1 aggregates (size 100 to 280 nm) in H1299 p53$^{-/-}$ cells with *C. trachomatis* infection and overexpression of p53 before or after (red arrow) infection. Number of Drp1 aggregates per cell (± SD) for noninfected cells, 3.4 ± 2.24; *C. trachomatis* (36 h), 3 ± 1.73; p53 OE, 882.3 ± 124.82; p53 OE + *C. trachomatis* (26 h), 790 ± 171.53; and *C. trachomatis* (36 h) ± p53 OE, 714.6 ± 215.07. Approximately 30 cells were analyzed from random selection of 20 regions of interest (ROIs) in each sample. Significance was determined by Mann–Whitney test; n = 3. (E) Graph represents colocalization analysis between Drp1 and mitochondrial GFP using the COLOC2 plugin. Pearson's correlation coefficient (R^2) values closer to 1.0 indicate strong positive correlation, whereas values closer to 0 indicate little or no discernable colocalization. Approximately 30 cells analyzed per sample; 2 or 3 random 10 × 10-µm ROIs were chosen in each selected cell; n = 3. (F) Immunoblot of infectivity assays of 36 h of primary *C. trachomatis* infection in HUVECs transfected with miR-30c mimic and p53 overexpression vector postinfection or preinfection. All data represent mean ± SD. Asterisks denote significance by unpaired t test. **, P < 0.01; ***, P < 0.001; ns, nonsignificant.

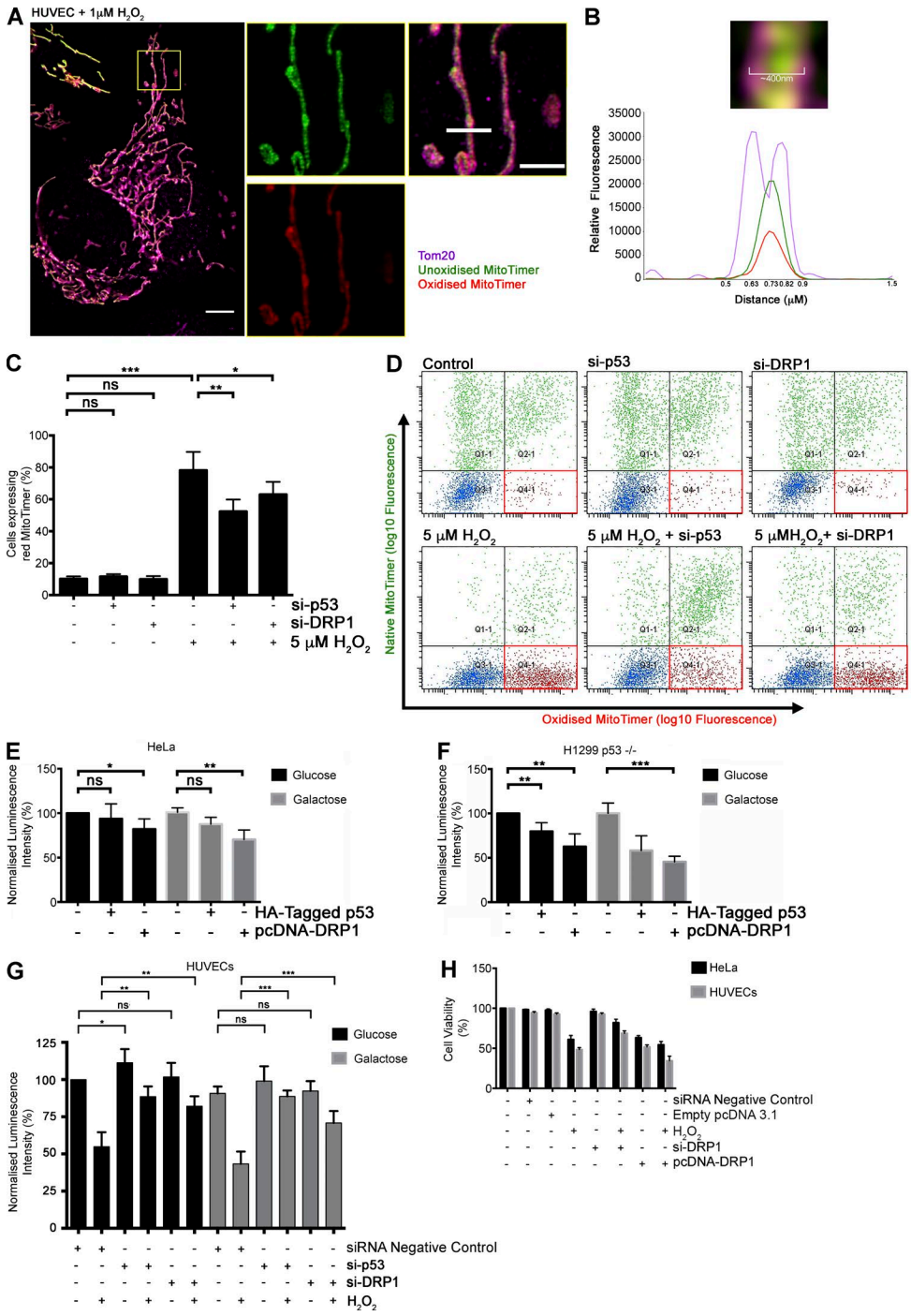

Figure S4. **Matrix localization of MitoTimer; effect of artificial modulation of DRP1 and p53 on MitoTimer oxidation; ATP abundance of HeLa, H1299 p53$^{-/-}$, and HUVECs; and effect of H_2O_2 and Drp1 depletion and overexpression on the cell viability of HUVECs and HeLa cells.** (A) Structured illumination micrograph of HUVECs expressing MitoTimer treated with 1 μM H_2O_2 for 15 min. The outer mitochondrial membrane (OMM) of the mitochondrial network has been stained with Tom20 to differentiate the OMM from the mitochondrial matrix. Bar, 5 μm. The 5 × 5-μm insets (yellow bordered) show the nonoxidized (green) and oxidized (red) form and the OMM marker Tom20 (purple). The last inset is the merged image with a 1.5-μm horizontal bar traversing the mitochondria. (B) Graph represents the intensity profile plot for nonoxidized and oxidized form of MitoTimer and Tom20 plotted along the 1.5-μm bar traversing the mitochondria (inset). (C and D) Graph and scatter plots represents quantification of the percentage of cells expressing the oxidized (red) form of MitoTimer in HUVECs transfected with siRNA negative control and siRNAs against p53 and Drp1 (separately) and/or treated with 5 μM H_2O_2 for 15 min (n = 3). (E and F) Graph represents quantification of total endogenous ATP levels in HeLa and H1299 p53$^{-/-}$ cells transfected with Drp1 overexpression vector or empty vector control. Indicated samples were incubated in glucose-free, galactose-supplemented medium and tested using a luminescent ATP detection kit according to the manufacturer's protocol. ATP luminescence was normalized to ATP levels of untreated and untransfected cells grown in glucose medium (n = 3). (G) Graph represents quantification of total endogenous ATP levels in HUVECs transfected with siRNA negative control and siRNAs against p53 and Drp1 (separately) and/or treated with 5 μM H_2O_2 for 15 min (n = 3). (H) HUVECs and HeLa cells were transfected with siRNA negative control or empty vector control, pcDNA-Drp1 overexpression vector, or Drp1 siRNA. Indicated samples were treated with 1 μM H_2O_2, and comparative cellular viability was measured using an MTT-based colorimetric assay (n = 10). All data represent mean ± SD. Asterisks denote significance by unpaired t test. *, P < 0.05; **, P < 0.01; ***, P < 0.001; ns, nonsignificant.

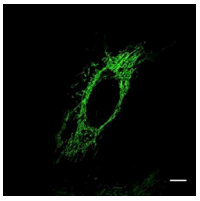

Video 1. **HUVECs expressing mitochondrially targeted Timer protein.** Related to Fig. 6. HUVECs transfected with pcDNA-MitoTimer expressing the unoxidized (green) form of the Timer protein within the mitochondrial network 24 h after transfection. Images were analyzed by time-lapse confocal microscopy using a laser-scanning confocal microscope (TCS SP5; Leica Biosystems). Frames were captured every minute for 30 min, and cells were imaged simultaneously in green (500 nm) and red (596 nm) channels. Bar, 10 µm. The video is displayed at 15 fps.

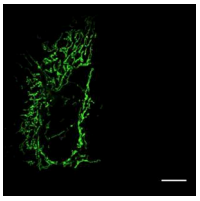

Video 2. **HUVECs expressing mitochondrially targeted Timer protein shifts its fluorescence spectrum upon H_2O_2 treatment.** Related to Fig. 6. Video shows the fluorescent spectrum shift of the MitoTimer protein from the unoxidized (green; 500 nm) form to oxidized form (red; 596 nm) upon addition of H_2O_2 (5 µM) to the imaging media. HUVECs transfected with pcDNA-MitoTimer for 24 h were imaged for 2 min (1 frame/min) before addition of H_2O_2 and then monitored by time-lapse confocal microscopy for 28 min (1 frame/min). The cells were imaged simultaneously in green (500 nm) and red (596 nm) channels. Bar, 10 µm. The video is displayed at 15 fps.

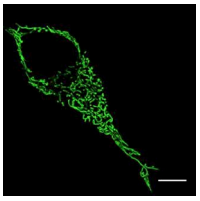

Video 3. **HUVECs expressing mitochondrially targeted GFP exhibit normal mitochondrial motility in absence of infection or H_2O_2 treatment.** Related to Fig. 7. Mito-HUVECs (green) were imaged for mitochondrial motility by time-lapse confocal microscopy using a laser-scanning confocal microscope (TCS SP5; Leica Biosystems). Frames were captured every 6 s for 5 min, and cells were imaged simultaneously in green (500 nm) and red (596 nm) channels. Bar, 10 µm. The video is displayed at 15 fps.

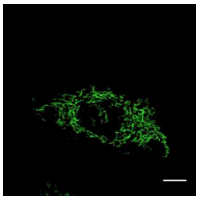

Video 4. **HUVECs expressing mitochondrially targeted GFP exhibit rapid fragmentation and enhanced fragment speed after H_2O_2 treatment.** Related to Fig. 7. Mito-HUVECs stably expressing mitochondrially targeted GFP (green) were treated with 1 µM H_2O_2 for 1 h and imaged by time-lapse confocal microscopy. The mitochondrial network under goes severe fragmentation, and the smaller fragments rapidly dissociate from the mitochondrial network. Frames were captured every 6 s for 5 min, and cells were imaged simultaneously in green (500 nm) and red (596 nm) channels.

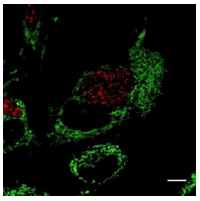

Video 5. **HUVECs infected with *C. trachomatis* exhibit dense mitochondrial network.** Related to Fig. 7. Mito-HUVECs stably expressing mitochondrially targeted GFP (green) were infected with *C. trachomatis* expressing mCherry for 30 h and imaged by time-lapse confocal microscopy. The infected cells exhibit dense and convoluted mitochondrial networks. Frames were captured every 6 s for 5 min, and cells were imaged simultaneously in green (500 nm) and red (596 nm) channels. The video is displayed at 15 fps.

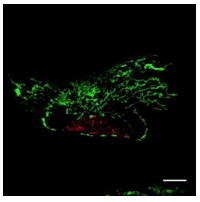

Video 6. **HUVECs infected with *C. trachomatis* resist H_2O_2-induced mitochondrial fragmentation.** Related to Fig. 7. Mito-HUV ECs stably expressing mitochondrially targeted GFP (green) were infected with *C. trachomatis* expressing mCherry for 30 h and treated with 1 µM H_2O_2 1 h before imaging. Infected cells exhibit unfragmented mitochondrial network and normal mitochondrial motility. Frames were captured every 5 s for 5 min, and cells were imaged simultaneously in green (500 nm) and red (596 nm) channels. The video is displayed at 15 fps.

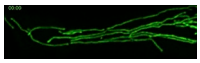

Video 7. **Noninfected HUVECs exhibit an almost equal number of fusion and fission events.** Related to Fig. 8. Mito-HUVECs (green) were imaged for mitochondrial motility by time-lapse confocal microscopy using a laser-scanning confocal microscope (Leica TCS SP5). Frames were captured every 5 min for 2 h and 55 min, and cells were imaged simultaneously in green (500 nm) and red (596 nm) channels. The video is displayed at 15 fps.

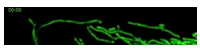

Video 8. ***C. trachomatis*–infected HUVECs exhibit slightly lower rates of fusion events and grossly decreased rates of fission events.** Related to Fig. 8. Mito-HUVECs stably expressing mitochondrially targeted GFP (green) were infected with *C. trachomatis* expressing mCherry for 30 h and imaged by time-lapse confocal microscopy. The infected cells steady elongation of the mitochondrial fragment in focus. Frames were captured every 5 min for 2 h and 55 min, and cells were imaged simultaneously in green (500 nm) and red (596 nm) channels. The video is displayed at 15 fps.

Provided online as a text file is the mitoCRWLR MACRO script. The MACRO script was used to analyze the mitochondrial mobility of the GFP-tagged mitochondrial particles within live cells. The MACRO script can be used on live cell video data using the FIJI image-processing platform.

Reference

Marin, M.C., C.A. Jost, L.A. Brooks, M.S. Irwin, J. O'Nions, J.A. Tidy, N. James, J.M. McGregor, C.A. Harwood, I.G. Yulug, et al. 2000. A common polymorphism acts as an intragenic modifier of mutant p53 behaviour. *Nat. Genet.* 25:47–54. http://dx.doi.org/10.1038/75586